Zero-Field Splitting of a ^6S Ion in Trigonal Symmetry

R. R. Sharma
Department of Physics, University of Illinois, Chicago, Illinois 60680
(Received 7 July 1969)

The expressions for various possible mechanisms under the point-multipole approximation which contribute to the zero-field splitting parameter D in the spin Hamiltonian $H_S = D[3S_z^2 - S(S+1)]$ for a paramagnetic ^6S ion in a trigonal symmetry have been derived. Important differences have been noticed in this axial symmetry in contrast with the results in the tetragonal symmetry considered previously. The applications of the expressions to two hypothetical cases and the real case of $CdCl_2:Mn^{2+}$ reveal that both the spin-spin and spin-orbit interactions are important. In the case of $CdCl_2:Mn^{2+}$, the spin-orbit contribution (-10.43×10^{-4} cm^{-1}) cancels a large part of the spin-spin contribution ($+15.35\times10^{-4}$ cm^{-1}), giving the value $D = +4.92\times10^{-4}$ cm^{-1}. This compares favorably with the results (at room temperature) of $< +5\times10^{-4}$ cm^{-1} for D from experiments on single crystals and $\sim +1\times10^{-4}$ cm^{-1} from experiments on powdered samples. The latter approximate result from powdered samples has been deduced by reducing the uncertainty in D using the graph illustrating the experimental variation of D with temperature. For $CdCl_2:Mn^{2+}$ it has also been pointed out that the value of D varies from -2.11×10^{-4} cm^{-1} to $+10.49\times10^{-4}$ cm^{-1} if one considers the existing uncertainty in the crystal structure parameter obtained from x-ray diffraction. In the present study, the presence of higher multipoles because of the ions, and the distortion of the lattice surrounding the magnetic ion, have not been taken into account.

I. INTRODUCTION

It has been shown recently[1-4] that the zero-field splitting of a ^6S transition metal ion in tetragonal and rhombic symmetries can be explained reasonably well on the basis of a point-charge point-multipole model. The following mechanisms involving spin-spin and spin-orbit interactions were treated in detail: (i) the Blume-Orbach (BO) mechanism,[1,3,5] (ii) the spin-spin (SS) mechanism proposed by Pryce,[6] (iii) the Orbach-Das-Sharma[7] (ODS) mechanism, and (iv) the Watanabe (W) mechanism[8] and also its corrected form in the presence of the cubic field (the WC mechanism). The contribution from the BO mechanism was found to be most dominant and the ODS and WC contributions, being of the same order of magnitude and opposite sign, were shown to nearly cancel each other.

Though the procedure used here is the same as given in Ref. 1, every step has to be repeated to make sure that the same relative phases of the wave functions and matrix elements have been retained throughout the work, since the functions in the trigonal systems are different and changes in relative phases may lead to wrong signs in various expressions for the splitting. Thus, in Sec. II we diagonalize the Hamiltonian containing free-ion terms in a cubic field in trigonal axes system to obtain the representations $^4\Gamma_4$ of the cubic field. One is required to repeat the diagonalization procedure here since different amplitudes and M_L values of ^4F and ^4G free-ion terms are now required to construct $^4\Gamma_4$ representations. Following the lines of Ref. 1 the quartet states are then admixed into the ^6S ground state via spin-orbit interaction. The expressions for D, the zero-field splitting parameter in the spin Hamiltonian

$$H_S = D[3S_z^2 - S(S+1)] \tag{1}$$

are then derived for BO mechanism in Sec. III. The ODS and WC mechanisms (and also W mechanism for comparison) are considered in Secs. IV and V, respectively. As regards the spin-spin contribution we use the expressions derived in tetragonal case, the explanation for which is given as follows.

The BO, ODS, and WC contributions are different in the present case than in tetragonal symmetry since, as mentioned above, different combinations of ^4F and ^4G states are now admixed into the ground state ^6S. On the other hand, the spin-spin mechanism as derived in the tetragonal case and the W mechanism neglect the presence of the cubic field and therefore do not involve the effects of cubic field admixtures of higher states. As shown in Ref. 1, the corrections to the W mechanism by the presence of the cubic field results in the WC mechanism. The spin-spin mechanism should also be corrected similarly. However, it can be shown that mixing of higher states by the cubic field into the ground state will not change the results drastically. In the presence of the cubic field the spin-spin contribution should be written as

$$D_{SS} \sim \langle {}^6S(3d^5) | H_{SS} | {}^6\Gamma \rangle' \tag{2}$$

instead of $\langle {}^6S(3d^5) | H_{SS} | {}^6S(3d^5) \rangle$ considered in Refs. 1 and 3. The state $|{}^6\Gamma\rangle'$ stands for the sextet rep-

resentations of the cubic field using a prime to show that they are perturbed to the first order by the axial field. The unperturbed $|{}^6\Gamma\rangle$ representations are linear combinations of the sextet terms (^6S, a^6D, z^6F^0, z^6P^0, etc.) of the free-ion[9] admixed by the cubic field. In Refs. 1 and 3 only the contribution from the lowest term ^6S was retained. This can be justified since the separations of higher sextet terms[9] from the ground state are about an order of magnitude larger than the cubic field splitting, thereby giving a negligible contribution to D. An important effect of this is that the spin-spin contribution remains the same in both trigonal and tetragonal cases as long as the axial field remains the same. In view of the above arguments one may use the expressions for D_{SS} written in Ref. 3 for calculations in trigonal symmetry.

The crystal fields required to estimate D for various mechanisms are given in Sec. VI. In order to assess the relative importance of different mechanisms, we first discuss two hypothetical cases in Sec. VII. One hypothetical case deals with the axial fields generated at a Mn^{2+} ion due to two single positive charges situated on a threefold axis of symmetry of the cubic field. The other hypothetical case is concerned with the axial fields produced on a magnetic ion by three single positive charges arranged on the vertices of an equilateral triangle, the plane of which is normal to a threefold axis of symmetry of the cubic field. In both cases it is important to remember that the magnetic ions are located in a cubic field and the axial fields are the perturbations over it. The first case should not be confused with the case of a single-charge considered in Ref. 1 where the charge lies on a fourfold axis of symmetry of the cubic field. These two cases represent different situations and therefore are not identical (even when the axial fields in both the cases happen to be equal). Section VII also includes theoretical estimates for a real case of Mn^{2+} in $CdCl_2$ where the results are compared and discussed in view of the available experimental data.[10,11] Sec. VIII is devoted to the conclusion.

II. DIAGONALIZATION IN A CUBIC FIELD AND PERTURBATION BY SPIN-ORBIT INTERACTION AND AXIAL FIELDS

The Hamiltonian of a $3d$ magnetic ion in a trigonal symmetry may be written as

$$H = H_0 + V_C + V_{SO} + V_{SS} + V_1^0 + V_2^0 + V_3^0 + V_4 \,. \tag{3}$$

The first term corresponds to the free-ion Hamiltonian and V_C is the cubic field (in trigonal axis system)

$$V_C = B_4^0 (4\pi/9)^{1/2} \textstyle\sum_i r_i^4 \{Y_4^0(i) + (\frac{10}{7})^{1/2} [Y_4^3(i) - Y_4^{-3}(i)]\} \,. \tag{4}$$

The terms V_{SO} and V_{SS} in Eq. (3) are the spin-orbit and spin-spin interactions. The fifth, sixth, and seventh terms, the axial crystal field terms of the first, second, and third degree, respectively, are

$$V_1^0 = - B_1^0 (4\pi/3)^{1/2} \textstyle\sum_i r_i Y_1^0(i) \,, \tag{5a}$$

$$V_2^0 = - B_2^0 (4\pi/5)^{1/2} \textstyle\sum_i r_i^2 Y_2^0(i) \,, \tag{5b}$$

$$V_3^0 = - B_3^0 (4\pi/7)^{1/2} \textstyle\sum_i r_i^3 Y_3^0(i) \,. \tag{5c}$$

The last term V_4 in Eq. (3) is the "unbalanced" axial field of the fourth degree,

$$V_4 = - (B_4^0)' (4\pi/9)^{1/2} \textstyle\sum_i r_i^4 Y_4^0(i) \,. \tag{6}$$

In this paper, we shall be concerned with a magnetic ion present in a trigonal symmetry especially where odd-degree crystal field terms do not survive. Therefore, one may ignore, at present, the presence of such terms as V_1^0 and V_3^0 in the Hamiltonian (3). However, such terms may be important for magnetic sites where these do not vanish; in those cases, the effect of these must be taken into account.

In order to perturb the ^6S ground state with spin-orbit interaction in the presence of the cubic field we use essentially the same treatment as given in Ref. 1 with the difference that the form of the representations of the cubic group $|L(^4\Gamma_4)M_\Gamma\rangle$ changes so as to correspond to the trigonal symmetry. The new functions $|L(^4\Gamma_4)M_\Gamma\rangle$ are listed in the Appendix. By comparing these functions with the corresponding functions in Ref. 1 one notes that different signs, amplitudes, and M_L values of the quartet states are required to construct these functions. For example, the functions $|G(^4\Gamma_4)1\rangle$ contain the sum $-(\frac{7}{8})^{1/2}|G1\rangle - (\frac{1}{8})^{1/2}|G-3\rangle$ in tetragonal symmetry against $-(\frac{4}{18})^{1/2}|G4\rangle + (\frac{7}{18})^{1/2}|G1\rangle + (\frac{7}{18})^{1/2}|G-2\rangle$ in trigonal symmetry.

Thus the spin-orbit admixed wave functions $|{}^6SM_S\rangle'$ in our case are the same in form as Eq. (14) of Ref. 1 with the important difference that the functions $|P(^4\Gamma_4)M_\Gamma\rangle$, $|F(^4\Gamma_4)M_\Gamma\rangle$, and $|G(^4\Gamma_4)M_\Gamma\rangle$ are appropriate to the trigonal symmetry as listed in the Appendix in terms of the states $|LM_L\rangle$ of a free ion. The wave functions $|{}^6SM_S\rangle'$ require the knowledge of the parameters $\alpha_i, \beta_i, \gamma_i, \Delta_i$, $a(M_S)$, $b(M_S)$, and $c(M_S)$, which must be recalculated in our case since the relative signs of these parameters (especially $\alpha_i, \beta_i, \gamma_i$) directly affect the signs of the terms in the expression for D in BO, ODS, and WC mechanisms (which involve the effects of cubic field mixing). It turns out that our calculations give the same values of α_i, β_i, γ_i, and Δ_i as given in Table I of Ref. 1 [and $a(M_S)$, $b(M_S)$, and $c(M_S)$ as in Table II in the same reference] if one uses the same values of the free-ion splittings and 10 Dq as given in Ref. 1. Though the values of these parameters have not altered in going from tetragonal to the trigonal case, it does not however mean

that the splitting parameter D from various mechanisms will not change from the tetragonal to the trigonal case.

For the ODS mechanism one also needs the perturbations by the axial field on the one-electron free-ion $3d$ states. These have already been obtained in Ref. 1 and may directly be used here (with a proper check that no wrong relative phase differences are introduced by doing so).

III. BO MECHANISM

The BO mechanism involves the first-order matrix element of an axial field between the spin-orbit admixed ground state $|{}^6S\ M_S\rangle'$ constructed in Sec. II. In trigonal symmetry both the second- and fourth-degree axial fields give nonvanishing contributions to the zero-field splitting. For purposes of comparison, we separate these parts. The first part, arising from the second degree crystal field, will be denoted by $D_{\mathrm{BO}\text{-}1}$. Thus, making use of Eqs. (29) and (30) of Ref. 1, with H_{ax} as given by Eq. (5b), one obtains

$$D_{\mathrm{BO}\text{-}1} = (\sqrt{5}/14)B_2^0 \langle r^2\rangle \zeta^2 p_{\alpha\beta} p_{\alpha\gamma}, \tag{7}$$

where the various symbols carry the same meanings as in Ref. 1.

The other part is derived in a manner analogous to the one given above but using Eq. (6) for the axial field H_{ax}. Denoting it by $D_{\mathrm{BO}\text{-}2}$, we have

$$D_{\mathrm{BO}\text{-}2} = -(\sqrt{5}/189)(B_4^0)' \langle r^4\rangle \zeta^2 p_{\alpha\gamma}(7p_{\alpha\alpha} + 4p_{\alpha\beta}), \tag{8}$$

again using the same symbols as in Ref. 1. It must be noticed that the BO-1 contribution [Eq. (7)] is finite here while it came out to be identically zero in tetragonal case (Ref. 1). The reason for this is the following. As mentioned in Sec. II, the functions $|L({}^4\Gamma_4)M_\Gamma\rangle$ involve different combinations of components $|{}^4LM_L\rangle$ of the quartet F and G states in the two cases. In other words, the mixing of these states by the cubic field is different along trigonal and tetragonal axes. The functions $|L({}^4\Gamma_4)M_\Gamma\rangle$ (and therefore different $|LM_L\rangle$ components of ${}^4F$ and ${}^4G$ states) are further admixed into one another by the application of the axial field [see Eq. (3) of Ref. 1]. In the tetragonal case the mixing is such that the contribution to D, as a result of mixing of $|{}^4G\pm 1\rangle$ and $|{}^4F\pm 1\rangle$ by the V_2^0 axial field, is equal and opposite to that from the mixing of $|{}^4G\pm 3\rangle$ and $|{}^4F\pm 3\rangle$ [see Eqs. (3) and (15) of Ref. 1]. Moreover, the other components $|{}^4LM_L\rangle$ do not get admixed by the axial field V_2^0 and hence do not contribute to the splitting. Consequently, the net splitting in tetragonal symmetry from the BO-1 mechanism vanishes. This is in sharp contrast with the situation in trigonal system where the charge density of $|L({}^4\Gamma_4)M_\Gamma\rangle$ states along the trigonal axis [compare expressions (A1) in the Appendix with the corresponding expressions in Ref. 1] is different than along the tetragonal axis in the previous case. As a result, the part of the splitting produced by the mixing of $|{}^4G\pm 1\rangle$ with $|{}^4F\pm 1\rangle$ by the axial field V_2^0 does not cancel that produced by the mixing of $|{}^4G\pm 2\rangle$ with $|{}^4F\pm 2\rangle$. Moreover, the contribution obtained by mixing $|{}^4G\pm 3\rangle$ with $|{}^4F\pm 3\rangle$ by V_2^0 does not vanish. Hence, the net splitting in trigonal symmetry from the BO-1 process comes out to be finite.

On account of the reasons associated with the charge density being different along the tetragonal and trigonal axes, it is not difficult to understand why we get different expressions for D in trigonal and tetragonal cases by the BO-2 process. On comparing Eq. (8) above and the corrected[3] Eq. (32) of Ref. 1 one finds that the coefficient of $p_{\alpha\alpha}p_{\alpha\gamma}$ has changed not only in magnitude but also in sign, whereas the coefficient of $p_{\alpha\beta}p_{\alpha\gamma}$ has changed in magnitude. The reasons in terms of the mathematical arguments are that (i) the matrix $\langle {}^4\Gamma_4\ 0|V_4|{}^4\Gamma_4 0\rangle$ vanishes in the tetragonal case while it is nonzero in the trigonal case; (ii) the matrix elements $\langle {}^4\Gamma_4\pm 1|V_4|{}^4\Gamma_4\pm 1\rangle$ have different values since in tetragonal case the contribution comes from $\langle {}^4F\pm 3|V_4|{}^4G\pm 3\rangle$ while in trigonal case it comes from $\langle {}^4F\pm 2|V_4|{}^4G\pm 2\rangle$; and (iii) the relative signs and amplitudes of $|{}^4LM_L\rangle$ states constituting the quartet Γ_4 functions are different in the two cases. The change in sign of the term $p_{\alpha\alpha}p_{\alpha\gamma}$ is mainly due to different signs of the terms containing $|{}^4LM_L\rangle$ states.

Also, since this term is dominant in expression (8), the contribution of the BO-2 mechanism changes sign from the tetragonal to the trigonal situation. This point will be clear from the numerical values in Sec. VII.

IV. ODS MECHANISMS

This process involves terms proportional to the axial field and spin-orbit interaction contributing both in the second order. Following the procedure of Ref. 1,

$$D_{\mathrm{ODS}} = -(1/18\sqrt{5})(B_2^0)^2 \zeta^2 p_{\alpha\gamma}[2(M_2 - 4M_1 + 3M_0)p_{\alpha\alpha} + (14M_2 - 11M_1 - 3M_0)p_{\alpha\beta}]. \tag{9}$$

Here Eq. (5b) has been used for the axial field. The quantities M_m stand for

$$M_m = \sum_{l'=0,2,4} a_{ml'} \langle u_{3d}^0 |r^2| u_{d^{-1}l'}^{(1)}\rangle, \tag{10}$$

where the coefficients $a_{ml'}$ are defined in Eq. (37) of Ref. 1. For other symbols one may consult Ref. 1.

One again notes that both sign and magnitude of the coefficient of $p_{\alpha\alpha}p_{\alpha\gamma}$ in Eq. (9) have changed while only the magnitude of the coefficient of $p_{\alpha\beta}p_{\alpha\gamma}$ has changed from the tetragonal to the trigonal case

[compare Eq. (9) above and Eq. (35) in Ref. 1]. The reasons for this are similar to those discussed in Sec. III for the BO process. Concisely, both amplitudes and relative signs of the $|^4LM_L\rangle$ states of F and G terms appearing in the $^4\Gamma_4$ functions are responsible for such changes. One important point to be noted is that the matrix element $\langle {}^4G-2|\,V_2^0\,|{}^4F-2\rangle$ contributes additionally to the splitting in trigonal case while no such matrix element appears in the other case. This is the main reason why the coefficient of $p_{\alpha\beta}p_{\alpha\gamma}$ is quite different in the two cases. Finally, the term containing $p_{\alpha\alpha}p_{\alpha\gamma}$ is dominant in expression (9) (as will be seen in Sec. VII) and since it has changed sign from the tetragonal to the trigonal case, the ODS contribution changes sign from one case to the other, as it is true for the BO-2 contribution.

V. W AND WC MECHANISMS

The WC mechanism considers the admixture of $|^4P\rangle$, $|^4F\rangle$, and $|^4G\rangle$ states into the ground state by spin-orbit interaction. The axial field then admixes the $|^4D\rangle$ states into the spin-orbit perturbed ground state. Proceeding as before, one gets

$$D_{\mathrm{WC}} = -\frac{1}{70}\frac{\zeta^2}{\Delta_{\mathrm{DS}}}\langle r^2\rangle^2 (B_2^0)^2 \times[(p_{\alpha\alpha}-\tfrac{8}{21}p_{\alpha\beta})^2+\tfrac{800}{441}(p_{\alpha\beta})^2], \tag{11}$$

where the parameters used here have already been defined in Ref. 1. For comparison, we also give the expression which one obtains using the W mechanism:

$$D_{\mathrm{W}} = -\frac{1}{70}\frac{\zeta^2}{\Delta_{\mathrm{DS}}}\frac{\langle r^2\rangle^2}{\Delta_{\mathrm{PS}}^2}(B_2^0)^2, \tag{12}$$

with the symbols defined in Ref. 1.

One notes again that because of the different weights, signs, and values of M_L of $|^4LM_L\rangle$ in $^4\Gamma_4$ functions, one gets different expression for D_{WC} in trigonal case [compare Eq. (11) above with Eq. (27) of Ref. 1]. Since the relative weights of ^4P states have not changed in the trigonal case against the tetragonal case [see Eq. (A1) in the Appendix and Eq. (15) of Ref. (1)], the term containing $p_{\alpha\alpha}^2$ remains intact. Also the sign and weight of $|^4F1\rangle$ state is responsible for changing the factor $\frac{4}{7}$ to $-\frac{8}{21}$ in Eq. (11). The last term in Eq. (11) appears because an additional matrix element $\langle {}^4D-2|\,V_2^0|{}^4F-2\rangle$ also contributes to the splitting in trigonal case. One may also note that the outside sign in expression (11) has not changed from the tetragonal to the trigonal situation, which is clear from the fact that D_{WC} involves absolute squares of matrix elements. The situation is not the same for BO − 2 and ODS contributions which have already been investigated in Secs. III and IV. This will be further clarified from the numerical values in Sec. VII.

VI. CRYSTAL FIELDS

As is clear from Eqs. (7)–(9), (11), and (12), one needs to evaluate the crystal fields (B_2^0) and $(B_4^0)'$ in order to estimate the zero-field splitting parameter D. In this section we give explicit expressions for these crystal fields. If the crystal fields are assumed to be generated by external point charges $q_j|e|$ located at (X_j, Y_j, Z_j) with the paramagnetic site as an origin, one has

$$B_2^0 = \textstyle\sum_j q_j(3Z_j^2 - R_j^2)/R_j^5\ , \tag{13}$$

$$(B_4^0)' = (B_4^0)_{nc} - \alpha(B_4^3)_{nc}\ , \tag{14}$$

where

$$\alpha = (B_4^0)_c/(B_4^3)_c\ , \tag{15a}$$

$$(B_4^0)_c = \frac{1}{4}\textstyle\sum_j^c q_j(35Z_j^4 - 30Z_j^2R_j^2 + 3R_j^4)/R_j^9, \tag{15b}$$

$$(B_4^3)_c = \frac{35^{1/2}}{2}\textstyle\sum_j^c q_jZ_jX_j(X_j^2 - 3Y_j^2)/R_j^9\ , \tag{15c}$$

$$(B_4^0)_{nc} = \frac{1}{4}\textstyle\sum_j^{nc} q_j(35Z_j^4 - 30Z_j^2R_j^2 + 3R_j^4)/R_j^9\ , \tag{16}$$

$$(B_4^3)_{nc} = \frac{35^{1/2}}{2}\textstyle\sum_j^{nc} q_jZ_jX_j(X_j^2 - 3Y_j^2)/R_j^9. \tag{17}$$

Here X_j, Y_j, Z_j, and R_j are in units of a_0, the Bohr radius; the parameter B_2^0 is in units of $e^2/2a_0^3$, and $(B_4^0)'$, $(B_4^0)_{nc}$, $(B_4^3)_{nc}$, $(B_4^0)_c$, and $(B_4^3)_c$ are in units of $e^2/2a_0^5$. In Eqs. (15) c stands for the cubic environment whereas in Eqs. (14), (16), and (17) nc designates the noncubic environment of the magnetic ion in a given host lattice. In writing the form of $(B_4^0)'$ [Eq. (14)] it has been assumed that the orientation of the X and Y axes relative to the Z axis (symmetry axis) is such that the cubic crystal field retains the form of Eq. (4). This is essential, as otherwise the effect of a part complementary to $(B_4^3)_{nc}$, that is,

$$(C_4^3)_{nc} = \frac{35^{1/2}}{2}\textstyle\sum_j^{nc} q_jZ_jY_j(Y_j^2 - 3X_j^2)/R_j^9 \tag{18}$$

must be accounted for to express $(B_4^0)'$ correctly. It will be seen that Eq. (18) gives vanishing results for the axes system we have chosen in Sec. VII. In that case one may use Eq. (14) directly to evaluate $(B_4^0)'$.

VII. RESULTS, COMPARISON WITH EXPERIMENT, AND DISCUSSION

The expressions derived in Secs. III–VI will now be employed to estimate the zero-field splitting parameter D in the following three different cases: (i) a hypothetical case which consists of two single-positive charges at the points $(0, 0, a)$ and $(0, 0, -a)$ with some appropriate value of a to produce a crys-

tal field at the origin where the magnetic ion (Mn^{2+}) is located; (ii) the case dealing with the axial symmetry at the magnetic ion at the origin where the axial crystal field is generated by three single-positive charges on the xy plane; and (iii) the case of the Mn^{2+} ion in $CdCl_2$. For all these cases the odd-degree crystal field terms vanish. The first two cases are investigated in order to assess the relative importance of various mechanisms in different environments of charges. The third case considers the real case of $CdCl_2:Mn^{2+}$ where experimental results are available for comparison.

For the evaluation of Eqs. (7) and (8) for D_{BO-1} and D_{BO-2}, one requires the values of $p_{\alpha\alpha}$, $p_{\alpha\beta}$, and $p_{\alpha\gamma}$. These may be obtained using their definitions and Table I in Ref. 1. One finds, in units of 10^{-5} cm, that $p_{\alpha\alpha}=3.821$, $p_{\alpha\beta}=-0.1327$, and $p_{\alpha\gamma}=1.295$ for $10\,Dq=10\,000\ cm^{-1}$. As regards the spin-spin coupling constant, one may assume that $\zeta=300\ cm^{-1}$ for Mn^{2+}. The values of $\langle r^2\rangle$ and $\langle r^4\rangle$ are calculated to be, respectively, 1.5482 and 5.5126 a.u. using Watson's Hartree-Fock functions for $3d$ electrons.[12] For D_{WC} and D_W [Eqs. (11) and (12)] one further needs the energy denominators which are taken as,[9] in units of $10^4\ cm^{-1}$, $\Delta_{DS}=3.2347$, $\Delta_{PS}=2.9205$. We will make use of these values for the parameters to estimate D from various mechanisms (BO, ODS, W, and WC) for all the three cases. As for the spin-spin contribution, as discussed in Sec. I, one may either use the relevant expressions from Ref. 3 or obtain it directly on multiplying the numbers under spin-spin mechanism in Table IV of the Appendix of Ref. 3 by the appropriate ratio of axial fields B_2^0.

A. Case I

This case considers the zero-field splitting of the Mn^{2+} ion at the origin due to perturbing axial fields created by two unit-positive charges placed on a threefold axis of cubic symmetry at a distance $4a_0$ from the origin, which may be thought of as a characteristic distance in crystals with trigonal symmetry. The present case must be compared with the case of a single charge considered in Ref. 1. The two cases are completely different since the charge distributions of the electronic cloud of a magnetic ion along [111] is not the same as along a [100] direction of a cubic crystal, especially when the axial fields (even though equal) are applied along these directions. The cubic field enters the picture because contributions from BO, ODS, and WC mechanisms involve $p_{\alpha\alpha}, p_{\alpha\beta}$, and $p_{\alpha\gamma}$, which depend on the strength of the cubic field and the probability of mixing quartet states into one another to form $^4\Gamma_4$ functions, which in turn depend on the strength of the cubic field.

As regards the crystal fields in the present case one finds from Eqs. (13)–(17) that $B_2^0=6.250\times10^{-2}$ and $(B_4^0)'=39.06\times10^{-4}$, where B_2^0 is in units of $e^2/2a_0^3$ and $(B_4^0)'$ in units of $e^2/2a_0^5$. Here, the value of α [Eq. (14)] is not effective since $(B_4^3)_{nc}$ vanishes. Using these values of B_2^0 and $(B_4^0)'$ the zero-field splitting parameter D for the BO, ODS, WC, and W mechanisms are then calculated from Eqs. (7)–(9), (11), and (12). The spin-spin contribution is quite straightforward to estimate from the relevant values in Ref. 3 and B_2^0 for the present case, as explained earlier. The contribution from the W mechanism is included just to compare with that from the WC mechanism. The calculated values of D from these mechanisms are listed in Table I. It is clear from this table that all the mechanisms contribute results of the same order of magnitude and are therefore equally important. One point to be noticed is that these mechanisms give the same relative sign to D. As regards the comparison between the WC and W mechanisms, the splitting from the WC mechanism comes out to be about 26% larger than that from the W mechanism. The ODS and WC mechanisms have the same relative signs and therefore they do not cancel each other as used to be the case in tetragonal and rhombic fields. Instead, they reinforce each other with the result that the sum of D_{ODS} and D_{WC}, namely, $-110\times10^{-4}\ cm^{-1}$ is almost equal to the total BO contributions ($-112\times10^{-4}\ cm^{-1}$).

Since the results in trigonal symmetry are profoundly different from tetragonal symmetry, it may be difficult for a reader to see how the results in these symmetries approach each other as the cubic field vanishes. The curves in Fig. 1 clarifiy this point, where the individual splittings from various

TABLE I. Results for the zero-field splitting parameter D in the spin Hamiltonian $H_S=D[3S_z^2-S(S+1)]$ arising from various mechanisms for two hypothetical cases and the case of $CdCl_2:Mn^{2+}$. (Values of D_W are included just for comparison with D_{WC}.)

D		Case I	Case II	$CdCl_2:Mn^{2+}$
D_{BO-1}		−26.24	+19.68	+8.82
D_{BO-2}		−85.40	−48.04	−6.80
D_{SS}[a]	$d\rightarrow s$	−32.62	+24.46	+10.96
	$d\rightarrow d$	+3.16	−2.37	−1.06
	$d\rightarrow g$	−16.22	+12.16	+5.45
	Total	−45.68	+34.25	+15.35
D_{ODS}		−42.92	−24.14	−4.85
D_{WC}		−67.32	−37.87	−7.60
D_W		−53.36	−29.56	−5.94
D(Total)		−267.56	−56.12	+4.92
D(Expt)				$<+5$[b]
				$\sim+1$[c]

[a]The spin-spin contributions may directly be obtained from Table IV of Ref. 3 by weighting with axial fields B_2^0 in various cases.

[b]Result from a single-crystal sample; see Ref. 10.

[c]Result from powdered sample; see Fig. 3 and Ref. 11.

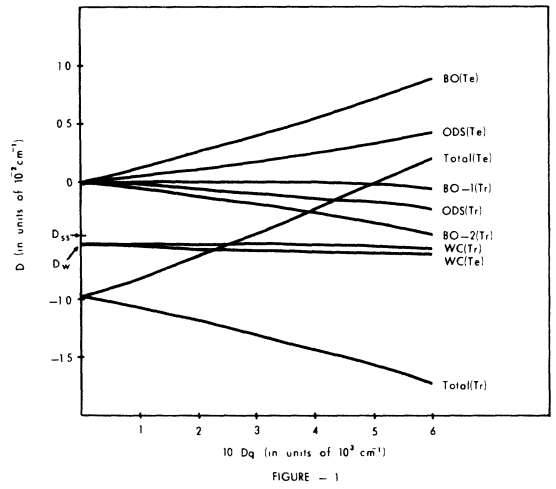

FIG. 1. Variation of D for various mechanisms as a function of 10 Dq in tetragonal (Te) and trigonal (Tr) symmetries corresponding to the crystal fields for Case I in text. "Total" designates the sum of the contributions from BO, ODS, WC, and SS mechanisms.

mechanisms and the total splitting are plotted as a function of 10 Dq in both tetragonal (Te) and trigonal (Tr) symmetries. When 10 Dq becomes zero, the BO and ODS contributions become zero, whereas the WC contribution approaches the W contribution in both symmetries. The W and SS values are marked on the left-hand side of the figure. The total contribution also approaches the sum of W and SS contributions in both symmetries.

B. Case II

In this case the perturbing axial field is assumed to be generated by three unit-positive charges placed in the xy plane on the vertices of an equilateral triangle where the z axis is a threefold symmetry axis of the cubic field in which the magnetic ion is located. The charges are assumed to be at a distance $4a_0$ from the magnetic ion at the origin (see Fig. 2). The crystal fields B_2^0 and $(B_4^0)'$ (Sec. VI) in this case are -4.688×10^{-2} (in units of $e^2/2a_0^3$) and 21.97×10^{-4} (in units of $e^2/2a_0^5$), respectively. The value of α (Eq. 14) is not required since $(B_4^3)_{nc}$

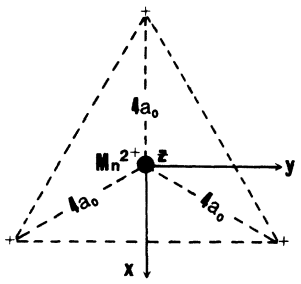

FIG. 2. Three positive-unit charges producing trigonal field at the Mn^{2+} ion.

vanishes in this case too. The results from various mechanisms may now be estimated using these values of B_2^0 and $(B_4^0)'$. The calculated values for D are listed in Table I. One notices again that the results from all the mechanisms are comparable. However, contrary to the conclusion from the first hypothetical case, the contributions D_{BO-1} and D_{BO-2} are opposite in sign. Also, the relative signs of D_{BO-1} and D_{SS} are the same, differing from the signs of D_{BO-2}, D_{ODS}, and D_{WC} (or D_W). Again, the WC mechanism is about 26% higher than the W mechanism. In contrast to the results of tetragonal and rhombic symmetry, but in agreement with the previous case, D_{ODS} and D_{WC} agree in sign and therefore do not cancel each other.

A comparison between the results obtained for the two hypothetical cases (see Table I) reveals that the total contribution to D has the same relative sign.

C. Case of $CdCl_2 : Mn^{2+}$

The crystal structure of $CdCl_2$ belongs to rhombohedral symmetry and space group D_{3d}^5 $(R\bar{3}m)$. Pauling and Hoard[13] have given crystal structure parameters from x-ray diffraction for a hexagonal unit cell of $CdCl_2$ which contains three molecules. These parameters together with the coordinates of the Cd^{2+} and Cl^- ions are listed in Table II. The successive Cd^{2+} layers in $CdCl_2$ crystal are separated by two Cl^- layers. As for the position of Cd^{2+} ions, they are situated in the octahedral holes

TABLE II. Crystal-structure data by Pauling and Hoard for a hexagonal unit cell of $CdCl_2$ containing three molecules.

a_H (in Å)	C_H (in Å)	u	Positions of Cd^{2+} ions	Positions of Cl^- ions
3.85	17.46	0.25 ± 0.01	$(0, 0, 0)$, $(\frac{1}{3}, \frac{2}{3}, \frac{1}{3})$, $(\frac{2}{3}, \frac{1}{3}, \frac{2}{3})$.	$(0, 0, u)$, $(0, 0, \bar{u})$, $(\frac{1}{3}, \frac{2}{3}, \frac{1}{3}+u)$, $(\frac{1}{3}, \frac{2}{3}, \frac{1}{3}-u)$, $(\frac{2}{3}, \frac{1}{3}, \frac{2}{3}+u)$, $(\frac{2}{3}, \frac{1}{3}, \frac{2}{3}-u)$.

between the nearest Cl^- layers. We attempt to interpret the zero-field splitting of the Mn^{2+} ion which substitutes for Cd^{2+} ion in the crystal. Though it is not strictly true, it will be assumed that the ions surrounding the Mn^{2+} ion occupy the same positions as they occupy in pure $CdCl_2$. It means that the lattice distortion effects due to the presence of the magnetic ion are neglected.

One may now compute the crystal fields B_2^0 and $(B_4^0)'$ from the expressions (13)–(17) and obtain D_{BO-1}, D_{BO-2}, D_{SS}, D_{ODS}, D_{WC}, and D_W. In order to assess the relative importance of various neighbors in explaining the splitting we first calculate the parameter D by considering successive neighbors starting with the first nearest up to the fourth nearest neighbors. The axes systems we have chosen are such that the Z axis lies along the crystal c axis [001], and Y axis along [100] with the X axis appropriately chosen to preserve the right-hand coordinate system. In Table III we list (i) the number of neighbors of a particular type (first nearest, second nearest, etc.), (ii) the distance of the neighbors from the Mn^{2+} ion, and (iii) the computed values of (B_2^0), and $(B_4^0)'$ using Pauling and Hoard's data (Table II) with $u = 0.25$. The parameter α needed to compute $(B_4^0)'$ [Eq. (14)] has been found to be $(\frac{7}{10})^{1/2}$ from Eqs. (15). From the crystal fields (B_2^0) and $(B_4^0)'$ it is easy to calculate D from various mechanisms. The calculated values are shown in Table III.

It may be observed from Table III, that the contribution due to the first and second nearest neighbors gives results with a negative sign. On the other hand, the contribution due to the third and fourth nearest neighbors is positive in sign. Besides this, the large contribution comes from the third and fourth nearest neighbors. It depicts, therefore, that a large number of surrounding ions must be taken into account to ensure correct value of D under point-charge approximation.

For estimating the crystal fields due to a sufficiently large number of surrounding ions we employ a method[4,14] of direct lattice summation. The method consists of dividing the crystal into different spherical shells about the magnetic ion with the radii na_H where $n = 1, 2, 3, \ldots$, etc., and a_H is the a dimension of the hexagonal unit cell of $CdCl_2$ (see Table II). Next, neutral groups each consisting of one Cd^{2+} ion and two Cl^- ions were formed in each crystal cell. For example, a neutral group consists of a central Cd^{2+} ion at (x, y, z) and two Cl^- ions at $(x, y, z+u)$ and $(x, y, z-u)$. Such a neutral group contributes to that shell in which the Cd^{2+} ion is located. Then, starting with the smallest shell the contributions to the crystal fields from larger shells were added up one by one until convergent results were obtained. The convergence is important in our case for estimating $(B_4^0)'$ correctly in Eq. (14), since it involves the difference of two large and nearly equal quantities $(B_4^0)_{nc}$ and $\alpha(B_4^3)_{nc}$. It is worth pointing out that the crystal field $(B_4^0)'$ accounts for the departure from the cubic field; it vanishes when the crystal symmetry is cubic.

In our calculations the crystal fields B_2^0 and $(B_4^0)'$ converge when one sums up the contributions from the shells within the radius $7a_H$. The computed results (using Table II with $u = 0.25$) from the neutral groups contained in the sphere of radius $7a_H$ are $B_2^0 = -8.107$, $(B_4^0)_{nc} = 35.5812$, $(B_4^3)_{nc} = 34.9475$, and $(B_4^0)' = 6.3421$, where B_2^0 is in units of $e^2/2a_H^3$ and the other crystal fields in units of $e^2/2a_H^5$. The parameter α needed for $(B_4^0)'$ [Eq. (14)] comes out to be $(\frac{7}{10})^{1/2}$ and the XYZ axes system used here has been described earlier. Just for comparison we also give results from spheres of radius $15a_H$: $B_2^0 = -8.091$, $(B_4^0)_{nc} = 35.5808$, $(B_4^3)_{nc} = 34.9473$, and $(B_4^0)' = 6.3418$, where again B_2^0 is in units of $e^2/2a_H^3$ and other crystal fields in units of $e^2/2a_H^5$.

Making use of the crystal fields (B_2^0) and $(B_4^0)'$ from sphere of radius $15a_H$ we now estimate D_{BO-1}, D_{BO-2}, D_{SS}, D_{ODS}, D_{WC}, and D_W. These are tabulated in Table I. Here again all the mechanisms are equally important. As seen in two hypothetical cases, it is also true in this case that the ODS and WC contributions are as large as other contributions. These two mechanisms have the same relative sign and therefore do not cancel each other. This differs from the results for tetragonal and rhombic symmetries. As regards the comparison between D_{WC} and D_W we notice again that the inclusion of the cubic field increases the W contribution by about 26%. The combined result of D_{BO-1} and

TABLE III. Calculated values of the crystal fields B_2^0 and $(B_4^0)'$ using Pauling and Hoard's crystal-structure data with $u = 0.25$ in $CdCl_2$ at Cd^{2+} site for first, second, third, and fourth nearest neighbors. B_2^0 is in units of $10^{-2}\ e^2/2a_0^3$ and $(B_4^0)'$ in units of $10^{-4}\ e^2/2a_0^5$. Also, D values are given in units of $10^{-4}\ cm^{-1}$.

Type of nearest neighbors	Number of nearest neighbors	Distance from Mn^{2+} in units of a_H	B_2^0	$(B_4^0)'$	D (total)
First	6	0.6898	0.4748	−1.533	−2.75
Second	6	1.0000	−3.116	4.415	−1.21
Third	2	1.1324	−0.7127	−1.047	+9.05
Fourth	12	1.5107	−0.6199	+0.5220	+4.91

D_{SS} gives a large positive value $+24.17\times10^{-4}$ cm^{-1}. On the other hand, the sum of D_{BO-2}, D_{ODS}, and D_{WC} gives a comparable negative value -19.25×10^{-4} cm^{-1}. The total from all these terms results in a small value[15], $+4.92\times10^{-4}$ cm^{-1}, for D, which compares with the corresponding results $<+5\times10^{-4}$ cm^{-1} (at room temperature) from the electron paramagnetic resonance experiment on a single crystal of $CdCl_2$ containing Mn^{2+} and $<+1\times10^{-4}$ cm^{-1} (at room temperature) from experiments on powdered $CdCl_2$.

Although the experiments at room temperature have not been able to give a definite value for D, it is possible to show that the experimental value lies close to $+1\times10^{-4}$ cm^{-1}. For this purpose we plot in Fig. 3 the experimental $3D$ values for various temperatures as obtained by Hoeve and Van Ostenburg.[11] Hoeve and Van Ostenburg give definite values for the D parameter at the temperatures (in °K) 20, 96, 510, 620, and 710. Perusal of Fig. 3 shows that the curve passes through a point close to $D=+1\times10^{-4}$ cm^{-1} at room temperature. This verifies that the experimental value of D is not very far from $+1\times10^{-4}$ cm^{-1} at room temperature. If this value is accepted as the experimental value of D our calculated result $+4.92\times10^{-4}$ cm^{-1} is in reasonable agreement with the experiment.

However, one notices that in Pauling and Hoard's crystal structure data (see Table II) the crystal parameter u is uncertain by the amount ±0.01. This forces us to estimate D for values of u lying between 0.24 and 0.26 in order to find how much D varies in this range of u. The crystal fields which we need to estimate D for different values of u may be computed by the method described earlier. The

TABLE IV. Crystal fields for different values (covering whole range of uncertainty) of the crystal parameter u using Pauling and Hoard's data. B_2^0 is in units of $10^{-2}\ e^2/2a_0^3$, $(B_4^0)_{nc}$ and $(B_4^3)_{nc}$ in units of $10^{-2}\ e^2/2a_0^5$, and $(B_4^0)'$ in units of $10^{-4}\ e^2/2a_0^5$.

u	B_2^0	$(B_4^0)_{nc}$	$(B_4^3)_{nc}$	$(B_4^0)'$
0.240	−2.951	0.1668	0.1368	5.251
0.242	−2.794	0.1691	0.1432	4.930
0.244	−2.630	0.1712	0.1501	4.559
0.246	−2.460	0.1728	0.1571	4.134
0.248	−2.284	0.1739	0.1642	3.653
0.250	−2.101	0.1745	0.1714	3.111
0.252	−1.911	0.1746	0.1788	2.506
0.254	−1.715	0.1741	0.1861	1.835
0.256	−1.513	0.1729	0.1936	1.095
0.258	−1.304	0.1710	0.2010	+0.2836
0.260	−1.088	0.1683	0.2084	−0.601

computed results for B_2^0, $(B_4^0)_{nc}$, $(B_4^3)_{nc}$, and $(B_4^0)'$ are given in Table IV for different values of u. It is now straightforward to estimate D using these crystal fields. The values of D as a function of u are depicted in Fig. 4. We find that D increases almost linearly with u from -2.11×10^{-4} cm^{-1} at $u=0.24$ to $+10.49\times10^{-4}$ cm^{-1} at $u=0.26$. It is interesting also to note from Fig. 3 that the value of u for which D becomes close to the experimental result $+1\times10^{-4}$ cm^{-1} is 0.2445. It is difficult to say whether this predicted value of u is the correct one unless one estimates the contributions from effects such as (i) overlap and charge-transfer covalency between the magnetic ion and the ligand ions, (ii) distortion of the lattice around the magnetic ion, and (iii) higher multipoles (dipoles, etc.) on the lattice. All of these effects may change our results significantly. However, it is clear that the parameter D experiences a large variation with a slight change in the value of u. One therefore needs a more exact value of u to compare the theoretical

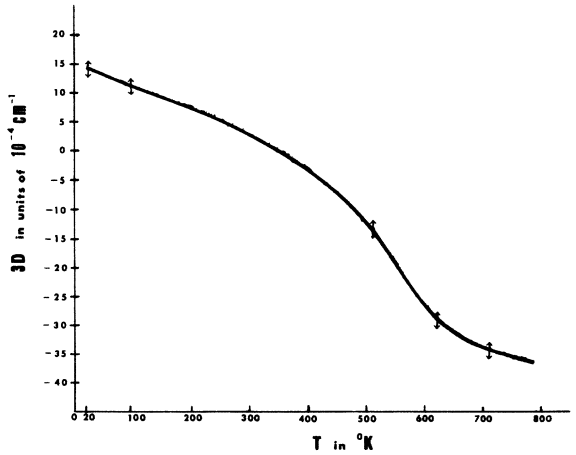

FIG. 3. Values of $3D$ as a function of temperature from the experimental data of Hoeve and Van Ostenberg (Ref. 11). The figure shows that the value of $3D$ lies close to $+3\times10^{-4}$ cm^{-1} at room temperature.

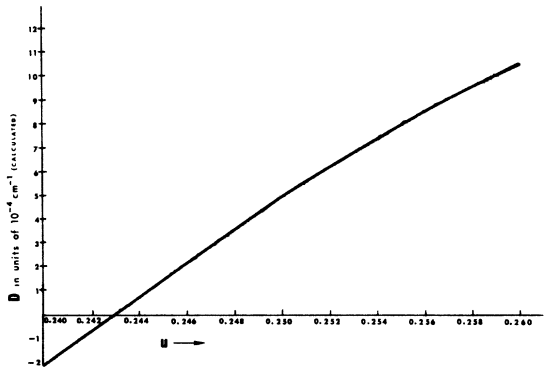

FIG. 4. Shows the change in the calculated value of D (in units of 10^{-4} cm^{-1}) for $CdCl_2:Mn^{2+}$ with the uncertainty in u, the crystal parameter.

value of D with the experimental results.

VIII. CONCLUSION

We have analyzed various mechanisms for the zero-field splitting of a ^6S ion in a trigonal symmetry starting with first principles and using a strictly external point-charge point-multipole model. The number of approximations has been kept as low as possible to obtain a realistic value of D. Our results for two hypothetical cases and for a real case of $CdCl_2$: Mn^{2+} show that all the mechanisms (BO, SS, ODS, and WC) are equally important. While the effect of the second degree axial potential in the BO process vanishes in the tetragonal and rhombic symmetries, it gives a definite contribution in trigonal symmetry. The ODS and WC mechanisms, in contrast to the situation for the splitting in tetragonal and rhombic symmetries, are of magnitudes comparable to other mechanisms (BO-1, BO-2, and SS). In addition, the ODS and WC mechanisms which used to cancel one another in tetragonal and rhombic symmetries are found here to enhance each other. Our calculated value of D, $+4.92\times10^{-4}$ cm^{-1} in $CdCl_2$: Mn^{2+} compares favorably with $<+5\times10^{-4}$ cm^{-1} from experiments on single crystals and lies close to $\sim+1\times10^{-4}$ cm^{-1} from experiments on powdered samples. However, it has been shown that the theoretical value of D changes from -2.11×10^{-4} cm^{-1} to $+10.49\times10^{-4}$ cm^{-1} as one takes into account the existing uncertainty in the value of the crystal-structure parameter u. A more exact value of the parameter u will be very helpful in deciding how far the theory can explain the experimental results.

In our calculations we have neglected the effects of overlap and charge transfer between the magnetic ion Mn^{2+} and the ligand ion Cl^-. Besides that, we have not taken into account the presence of higher multipoles (dipoles, etc.) on the ions and the distortion of the lattice surrounding the magnetic ion to calculate the crystal fields.

ACKNOWLEDGMENTS

The author is particularly grateful to Professor S. Sundaram for reading the manuscript very critically. Thanks are due to Dr. H. G. Hoeve and Dr. D. O. Van Ostenburg for very useful conversations. It is also a pleasure to acknowledge the assistance of Ashok K. Sharma in numerical calculations for Fig. 1.

APPENDIX

The functions $|P(^4\Gamma_4)M_\Gamma\rangle$, $|F(^4\Gamma_4)M_\Gamma\rangle$, and $|G(^4\Gamma_4)M_\Gamma\rangle$ used in Sec. II are listed in terms of the states $|LM_L\rangle$ of the $3d^5$ electrons as follows:

$$
\begin{aligned}
&|P(^4\Gamma_4)1\rangle = |P1\rangle,\\
&|P(^4\Gamma_4)0\rangle = |P0\rangle,\\
&|P(^4\Gamma_4)-1\rangle = |P-1\rangle,\\
&|F(^4\Gamma_4)1\rangle = -(\sqrt{6})^{-1}|31\rangle - (\tfrac{5}{6})^{1/2}|3-2\rangle,\\
&|F(^4\Gamma_4)0\rangle = -(\tfrac{5}{18})^{1/2}|33\rangle + (\tfrac{8}{18})^{1/2}|30\rangle + (\tfrac{5}{18})^{1/2}|3-3\rangle,\\
&|F(^4\Gamma_4)-1\rangle = -(\sqrt{6})^{-1}|3-1\rangle + (\tfrac{5}{6})^{1/2}|32\rangle, \qquad \text{(A1)}\\
&|G(^4\Gamma_4)1\rangle = -(\tfrac{4}{18})^{1/2}|44\rangle + (\tfrac{7}{18})^{1/2}|41\rangle + (\tfrac{7}{18})^{1/2}|4-2\rangle,\\
&|G(^4\Gamma_4)0\rangle = (\sqrt{2})^{-1}|43\rangle + (\sqrt{2})^{-1}|4-3\rangle,\\
&|G(^4\Gamma_4)-1\rangle = -(\tfrac{4}{18})^{1/2}|4-4\rangle - (\tfrac{7}{18})^{1/2}|4-1\rangle + (\tfrac{7}{18})^{1/2}|42\rangle,
\end{aligned}
$$

where for defining the phases we give ^4P, ^4F, and ^4G states with $M_L = L$, $M_S = S$:

$$
\begin{aligned}
|^4P1\rangle &= (\sqrt{5})^{-1}[\,|2^+1^+0^+ - 1^+ - 1^-\rangle + (\tfrac{3}{2})^{1/2}|2^+1^+0^+0^- - 2^+\rangle\\
&\quad + (\tfrac{3}{2})^{1/2}|2^+1^+1^- - 1^+ - 2^+\rangle + |2^+2^-0^+ - 1^+ - 2^+\rangle\,],\\
|^4F3\rangle &= (\sqrt{2})^{-1}[\,|2^+1^+1^-0^+ - 1^+\rangle + |2^+2^-1^+0^+ - 2^+\rangle\,],\\
|^4G4\rangle &= |2^+2^-1^+0^+ - 1^+\rangle. \qquad \text{(A2)}
\end{aligned}
$$

The other $|^4LM_L\rangle$ states needed in (A1) may be obtained from (A2) by means of lowering and raising operators.

[1] R. R. Sharma, T. P. Das, and R. Orbach, Phys. Rev. 149, 257 (1966).

[2] R. R. Sharma, T. P. Das, and R. Orbach, Phys. Rev. 155, 338 (1967).

[3] R. R. Sharma, T. P. Das, and R. Orbach, Phys. Rev. 171, 378 (1968).

[4] R. R. Sharma, Phys. Rev. 176, 467 (1968).

[5] M. Blume and R. Orbach, Phys. Rev. 127, 1587 (1962).

[6] M. H. L. Pryce, Phys. Rev. 80, 1107 (1950).

[7] R. Orbach, T. P. Das, and R. R. Sharma, in *Proceedings of the International Conference on Magnetism, Nottingham*, 1964 (The Institute of Physics and the Physical Society, London, 1965), p. 330.

[8] H. Watanabe, Progr. Theoret. Phys. (Kyoto) 18, 405 (1957).

[9] C. E. Moore, National Bureau of Standards Report No. 467 (U.S. GPO, Washington, D. C., 1949).

[10] H. Koga, K. Horai, and O. Maturmura, J. Phys. Soc. Japan 15, 1340 (1960).

[11] H. G. Hoeve and D. O. Van Ostenburg, Phys. Rev. 167, 245 (1968). For experimental data at 20° K in $CdCl_2$: Mn^{2+}, see also T. P. P. Hall, W. Hayes, and F. I. B. Williams, Proc. Phys. Soc. (London) 78, 883 (1961).

[12] R. E. Watson, Phys. Rev. 118, 1036 (1960).

[13] L. Pauling and J. L. Hoard, Z. Krist. 74, 546 (1930).

[14] R. H. Wood, J. Chem. Phys. 32, 1690 (1960).

[15] If one uses a $a_H = b_H = 3.854$ Å and $C_H = 17.457$ Å as given by Wyckoff [R. W. G. Wyckoff, *Crystal Structures* (Interscience, New York, 1960)], one gets instead a slightly different value of D, namely, $D = +5.04\times10^{-4}$ cm^{-1}.